Biophysical Chemistry, 31 (1988) 121–131
Elsevier

BPC 01291

Solution spatial structure of 'long' neurotoxin M_9 from the scorpion *Buthus eupeus* by ^{1}H-NMR spectroscopy

Vladimir S. Pashkov, Vladimir N. Maiorov, Vladimir F. Bystrov *, Anh N. Hoang, Tatyana M. Volkova and Eugene V. Grishin

Shemyakin Institute of Bioorganic Chemistry, U.S.S.R. Academy of Sciences, Ul. Miklukho-Maklaya, 16/10, 117871 GSP Moscow V-437, U.S.S.R.

Received 5 September 1987
Accepted 1 February 1988

Scorpion toxin; Neurotoxin M_9; NMR; Nuclear Overhauser effect; Protein conformation; (*Buthus eupeus*)

^{1}H-NMR spectra of *Buthus eupeus* neurotoxin M_9 (66 amino acid residues, four disulfide bonds) reveal two slowly exchangeable conformations at acidic pH. The spatial structure of the conformer prevailing under physiologically relevant conditions has been determined from two-dimensional ^{1}H-NMR data treated by means of a distance geometry algorithm and refined by molecular modelling. Interrelation between the structure and function of mammalian neurotoxin M_9 is discussed by comparing its conformation with those of the scorpion insectotoxins which exhibit different biological specificity (insectotoxins v-2, v-3 and I_{5A}).

1. Introduction

Scorpion venoms contain a set of polypeptide toxins which show different biological specificity [1]. All mammalian toxins and most of the insect toxins generally consist of 60–80 amino acid residues, while some insect toxins are composed of 35–36 residues (both structural groups contain four disulfide bridges) [1,2]. Similar crystal structures have been evaluated for two 'long' insectotoxins, v-2 and v-3, isolated from *Centruroides sculpturatus* [3,4] which differ only in three amino acid residues, and it has been shown [5] that the NMR spectra of an aqueous solution of v-3 do not contradict with the crystal structure. The solution conformation of 'short' insectotoxin I_{5A} from *Buthus eupeus* has been determined by ^{1}H-NMR spectroscopy [2,6–9]. As far as mammalian scorpion toxins are concerned, structural information is limited to theoretical predictions [4] and experimental data on conformational transitions [10].

This paper deals with elucidation of the spatial structure in solution of *B. eupeus* scorpion neurotoxin M_9 (active on mammals) by NMR spectroscopy data treated by a modified distance geometry algorithm [9] and molecular model refinement. The toxin consists of 66 amino acid residues with four disulfide bonds [11]. Like many other mammalian and scorpion toxins, it acts on the Na^+ channels of excitable membranes and interferes with their normal functioning [2].

Correspondence address: V.F. Bystrov, Shemyakin Institute of Bioorganic Chemistry, U.S.S.R. Academy of Sciences, Ul. Miklukho-Maklaya, 16/10, 117871 GSP Moscow V-437, U.S.S.R.

Abbreviations: M_9, *Buthus eupeus* neurotoxin M_9; v-2 and v-3, *Centruroides sculpturatus* Ewing insectotoxins v-2 and v-3, respectively; $I_{5\bar{A}}$, *B. eupeus* insectotoxin I_{5A}; NOE, nuclear Overhauser effect.

2. Materials and methods

Neurotoxin M_9 was isolated from the venom of the Central Asian scorpion *B. eupeus* as described in ref. 11.

NMR samples were prepared using doubly distilled ^1H_2O or ^2H_2O (99.5–99.8% deuterium, Iso-

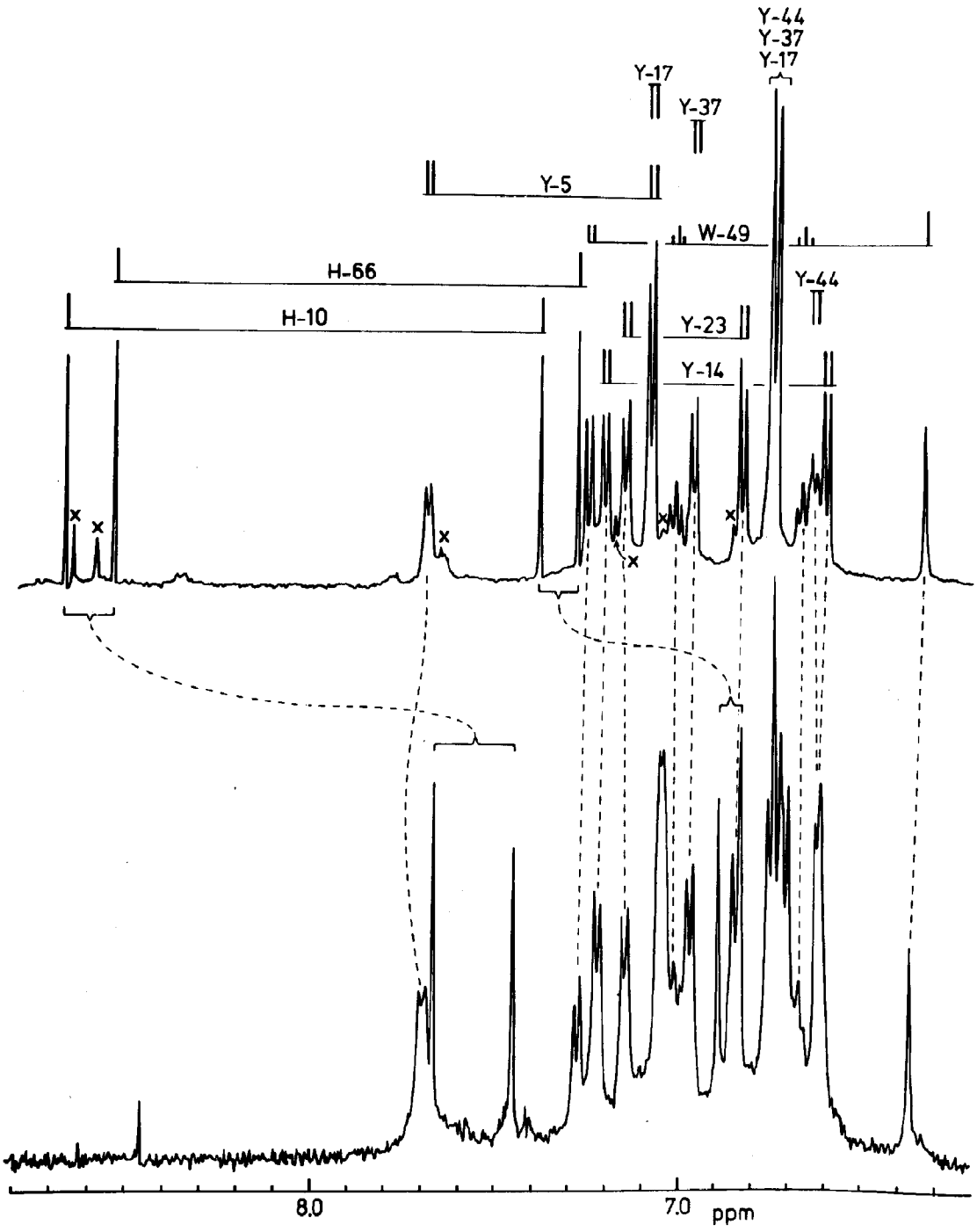

Fig. 1. Aromatic region of the one-dimensional ^{1}H-NMR spectra of neurotoxin M_9 in ^2H_2O at 32°C; pH 2.6 (top) and pH 10.0 (bottom). Vertical lines and x indicate respective signals of the dominant and minor conformers at pH 2.6. Broken lines connect the same dominant conformer signals at different pH values. Signals of the dominant conformer are identified with the residue type (using the single-letter code) and its positional number in the sequence.

top, U.S.S.R.; or 99.96–100% deuterium, Stohler Isotope Chemicals). The pH values correspond to the direct reading of an Orion Research 601 pH-meter fitted with a 180 mm Ingold M3 combined electrode. The pH values were measured directly in NMR sample tubes (5 mm outer diameter) at room temperature. To alter the pH, 0.15 or 1.5 M solutions of ^{2}HCl and KO^{2}H, which were prepared from ^2H_2O and ^{2}HCl (38% in ^2H_2O, 99% deuterium; Stohler) or KO^{2}H (40% in ^2H_2O, 98% deuterium; Stohler) were used.

The one-dimensional ^{1}H-NMR spectra were obtained for 0.7 mM solutions of M_9 in ^2H_2O. The two-dimensional ^{1}H-NMR (COSY or NOESY) spectra were acquired for 3 or 5 mM solutions of M_9 in ^2H_2O or a $^1H_2O/^2H_2O$ (9:1) mixture, respectively. Prior to experiments in ^2H_2O labile protons of M_9 were exchanged by freeze-drying of the M_9 solution in ^2H_2O and redissolving the material in ^2H_2O.

The ^{1}H-NMR spectra were recorded at 500 MHz using a Bruker WM-500 spectrometer equipped with an Aspect 2000 or Aspect 3000 computer using conventional software (FTQNMR, DISN83, DISN85, DISR86) in the pulsed Fourier-transform mode with quadrature mode detection. To record one-dimensional and two-dimensional ^{1}H-NMR (COSY and NOESY) spectra, the following pulse sequences were used, respectively: $(t_0\text{–}90°\text{–}t_2)_n$, $(t_0\text{–}90°\text{–}t_1\text{–}90°\text{–}t_2)_n$, $(t_0\text{–}90°\text{–}t_1\text{–}90°\text{–}\tau_m\text{–}90°\text{–}t_2)_n$ where t_0 is the preparation period (1–3 s for one-dimensional and 1.2 s for two-dimensional spectra), t_2 the observation period (0.7–1.3 s for one-dimensional and 0.33–0.41 s for two-dimensional spectra), τ_m the mixing time (0.2 s), t_1 the evolution period (512 different t_1 values used) and n the number of accumulations (600–1500 times for one-dimensional and 136–256 times for each t_1 of the two-dimensional spectra).

The two-dimensional ^{1}H-NMR spectra were acquired in the phase-sensitive mode with quadrature detection in the t_1 dimension exept for the NOESY spectra in ^2H_2O, where the carrier frequency was displaced from the centre of the spectrum to the low-field side and quadrature detection in the t_1 dimension was not used [12]. For experiments with quadrature detection, the spectral width was 6250 Hz in both ω_1 and ω_2 dimensions (4096 data points accumulated in the t_2 dimension). For the NOESY spectrum in ^2H_2O, the spectral width was 10000 Hz in the ω_2 dimension and 5000 Hz in the ω_1 dimension (8192 data points accumulated in the t_2 dimension).

Prior to Fourier transformation, the time-domain data were multiplied by window functions, then extended by zero filling (i.e., to increase sensitivity, the number of data points in the t_2 dimension was often reduced or replaced by zero points). Both phase-sensitive and absolute-value data were used. After Fourier transformation, the digital resolution was 0.8–3 Hz/point for the one-dimensional spectra. A digital resolution of 5–6 Hz/point was obtained in both dimensions (ω_1 and ω_2) of the absolute-value mode two-dimensional spectra, and in the ω_1 dimension of the phase-sensitive two-dimensional spectra. For the ω_2 dimension of the phase-sensitive two-dimensional spectra, the digital resolution was 0.4–3 Hz/point.

The coupling constants ^3J(H-NC$^\alpha$-H) were measured from the NH proton cross-peak splittings in suitably selected cross-sections along the ω_1 axis of the phase-sensitive COSY and/or NOESY spectra.

The slowly exchanging peptide NH protons were identified from their cross-peaks that re-

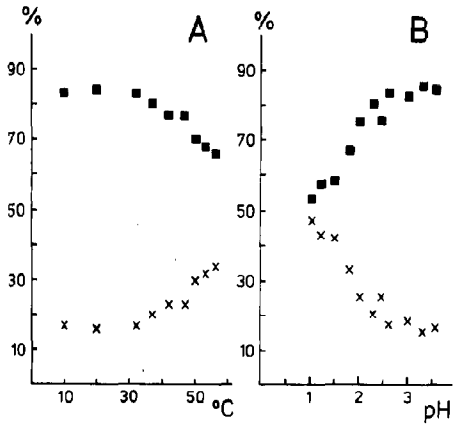

Fig. 2. Dependence of the relative proportions of the major (■) and minor (×) conformers of neurotoxin M_9 on (A) temperature (at pH 2.6), and (B) pH (at 32°C), calculated from the relative intensity of the C2-H proton signals of residues His-10 and His-66.

mained in the combined COSY and NOESY spectra [13], acquired over 31 h using a 9 mM solution of M_9 in ^2H_2O at pH 2.5 and 30 °C, after incubation of the sample under the same conditions for 14 h. These spectra were acquired using spectral widths of 12 500 Hz in the ω_2 dimension and 6250 Hz in the ω_1 dimension. The carrier was placed on the low-field side of the spectrum and the spectra were acquired with quadrature detection in the ω_2 dimension only. For both spectra, 512 t_1 and 4096 t_2 data points were acquired. Further data processing was carried out in the absolute-value mode.

All ^{1}H-NMR spectra were acquired with selective, continuous irradiation of the solvent resonance at all times, except during data acquisition. Chemical shifts are expressed in ppm downfield from internal DSS (4,4-dimethyl-4-silapentane-1-sulfonate).

3. Results

The one-dimensional ^{1}H-NMR spectra of neurotoxin M_9 were recorded over a limited pH range because of the low solubility within the pH range 3.5–9.0 and irreversible denaturation at pH > 11.5 (32 °C). The pH dependence provides a rough estimation of the pK_a values of the His-10 and His-66 imidazole rings ($5 < pK_a < 7$) and reveals the existence of two conformers of M_9 at acidic pH. The conformational heterogeneity is most clearly seen for the well-resolved C2-H resonances of residues His-10 and His-66. Each of the resonances is split into two peaks (fig. 1). As estimated from the linewidths of these peaks, the rate of conformer interconversion is $< 5\ s^{-1}$. The pH dependence of the relative concentrations of both M_9 conformers (fig. 2) presumably indicates that the conformational heterogeneity of the molecule

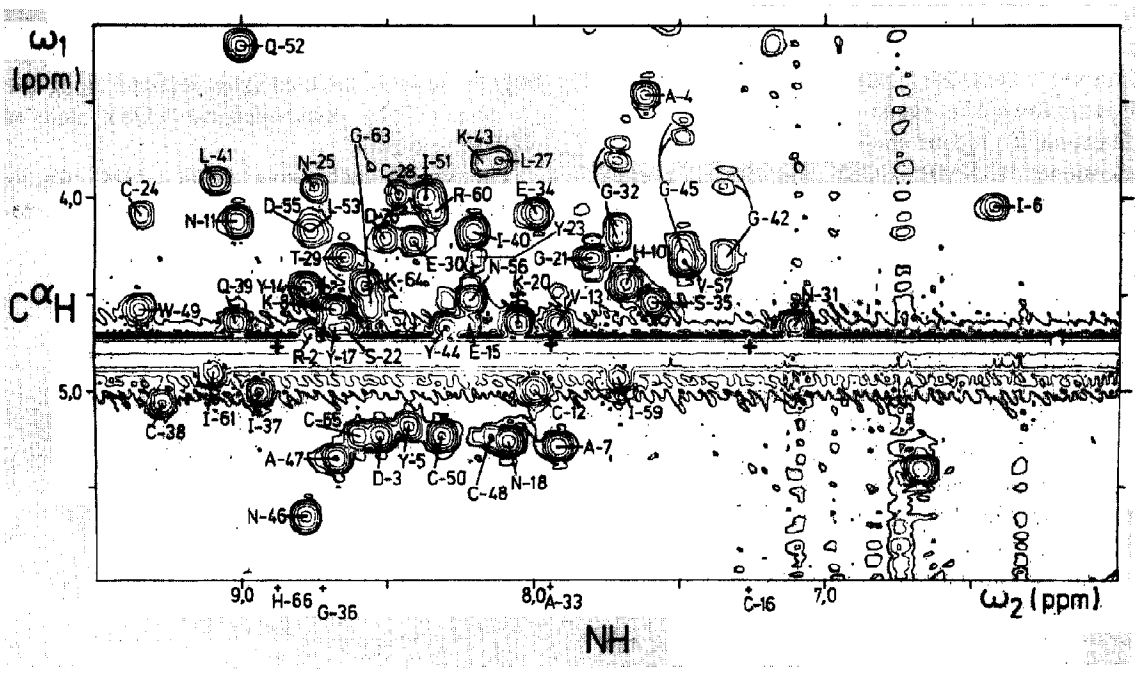

Fig. 3. Contour plot of the region $\omega_1 = 3.1$–6.0 ppm, $\omega_2 = 6.0$–9.5 ppm of the absolute-value mode COSY proton spectrum of neurotoxin M_9 in a $^1H_2O/^2H_2O$ (9:1) mixture at 30 °C and pH 3.0. The strong horizontal noise band at 4.7 ppm is due to water, which was suppressed by selective irradiation. The NH-C$^\alpha$H cross-peaks identified in the spectrum are indicated, while those which were not distinguished are shown by crosses. The chemical shifts of the corresponding NH protons and their assignment are shown at the bottom of the plot.

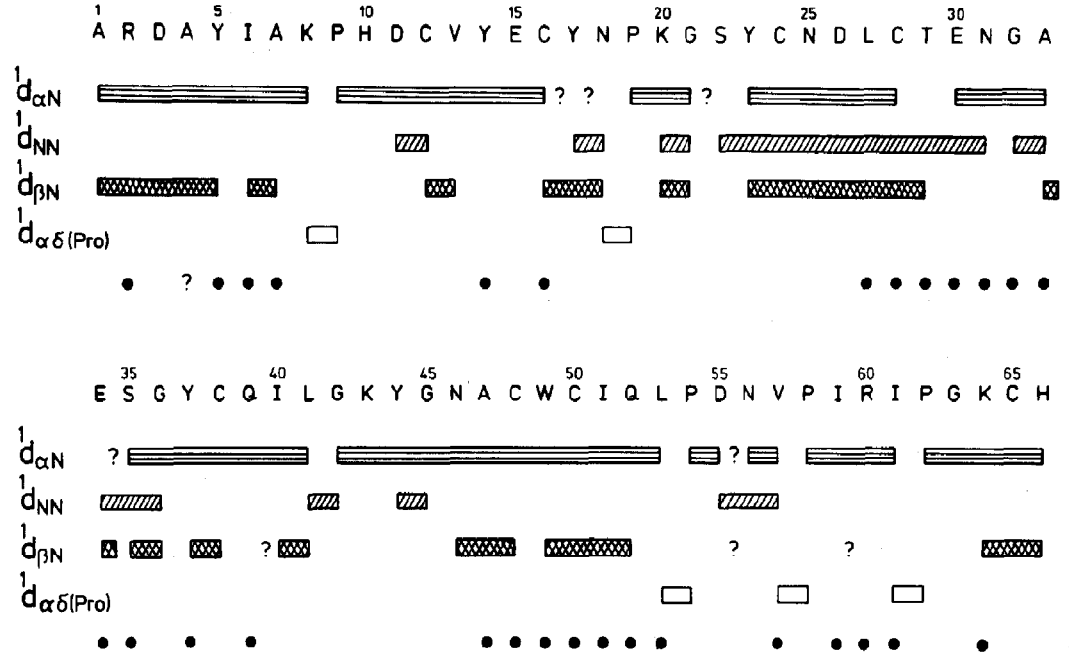

Fig. 4. Primary structure of neurotoxin M_9. Rectangular bands represent the experimentally observed NOE interactions $^1d_{xy}$ (see footnote to table 1). Filled circles indicate slowly exchanging peptide NH protons. Question marks designate ambiguous experimental data.

is due to the protonation of one or more carboxyl groups with $pK_a \sim 2$. In alkaline medium (pH > 10) the spectrum corresponds to only one structural form.

The two-dimensional ^{1}H-NMR spectra of the M_9 conformer, which predominates under physiologically relevant conditions, were recorded at pH 2.5–3.0 and 30 °C. Under these conditions, M_9 is sufficiently soluble and the conformational equilibrium is substantially shifted towards the conformer of interest (> 80%, fig. 2), so that cross-peaks of the other conformer merge with the noise in the two-dimensional spectra of M_9.

Identification of the two-dimensional spectral signals commenced from the NH-C$^\alpha$H cross-peak region of the COSY spectrum (fig. 3) of M_9 in $^1H_2O/^2H_2O$ (9:1). This region is often called the NMR 'fingerprint' of a protein molecule [14], since each amino acid residue is represented in it by one cross-peak with the exception of N-terminal and proline residues (both absent) and glycine residues (two cross-peaks per residue). Most of the NH-C$^\alpha$H cross-peaks expected, according to the amino acid composition of M_9, were identified in the COSY spectrum (figs. 3 and 4). Assignment of cross-peaks belonging to the individual amino acid residues was performed by analysing two-dimensional spectra (COSY and NOESY). This task was greatly simplified because phase-sensitive two-dimensional spectra were obtained which, as shown in ref. 15, substantially diminish the ambiguity in cross-peak assignment. Most of the proton spin-systems were differentiated according to amino acid residue type, before assignment of the individual amino acid residue spin-systems to specific positions in the primary structure. The final assignments were accomplished by means of the conventional procedure of sequential resonance assignment through dipole-dipole interactions of the NH proton (C$^\delta$H$_2$ or C$^\alpha$H for proline residue only [8]) of residue $i+1$, with the C$^\alpha$H, NH and C$^\beta$H protons of the preceding residue, i [16] (fig. 4).

By analysis of the COSY and NOESY spectra

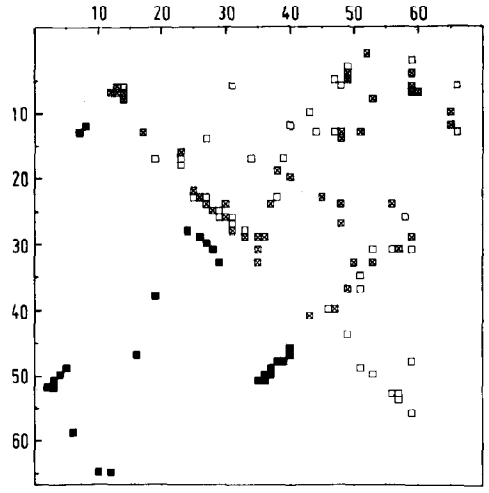

Fig. 5. NOE contact map of neurotoxin M_9. Amino acid sequence numbers are plotted along the axes. Filled squares below the diagonal indicate backbone-backbone contacts. Crossed and empty squares above the diagonal indicate backbone-side chain and side chain-side chain contacts, respectively. In cases where positions of crossed and empty squares coincide, only the crossed square is shown. Each contact is indicated only once above or below the diagonal line.

almost all proton signals from all amino acid residues of the dominant conformer of M_9 were assigned according to the primary structure [17]. Under the conditions employed for NOESY experiments (mixing time 0.2 s), nuclear Overhauser effect (NOE) cross-peaks correspond to protons separated by less than 0.5 nm [18]. About 1000 NOEs were detected between the different proton pairs of M_9. Some are presented in figs. 4, 5 and 7–9 and table 1.

To evaluate the spatial structure of neurotoxin M_9, the NMR data obtained were treated by means of a modified distance geometry algorithm [9,19], with simplified representation of an amino acid residue by two spherical pseudoatoms α and

Table 1

NOE interactions ($^nd_{xy}$) [a] [20] indicative of standard regular secondary structures established in the NOESY spectra of M_9

$\cdots$–NH–C$^\alpha$H(C$^\beta$H <)–CO–$\cdots$–NH–C$^\alpha$H(C$^\beta$H <)–CO–$\cdots$

i $\longleftarrow$ $^nd_{xy}$ $\longrightarrow$ $i+n$

NOE interaction	Amino acid residues i–($i+n$)
α-Helix (residues 22–31)	
$^3d_{\alpha N}$	23–26, 24–27, 26–29, 27–30, 28–31
$^3d_{\alpha\beta}$	22–25, 23–26, 24–27, 25–28, 28–31
$^4d_{\alpha N}$	24–28
β-Sheet (residues 1–5, 46–52, 35–40)	
$^nd_{NN}$	2–52, 4–50, 35–51, 37–49
$^nd_{\alpha\alpha}$	3–51, 5–49, 36–50, 38–48
$^nd_{\alpha N}$	3–52, 36–51, 40–47
$^nd_{N\alpha}$	4–51, 37–50, 39–48, 41–46

[a] Subscripts (x and y) indicate atoms to which protons under consideration are attached; i designates the position of the amino acid residue in the primary structure of M_9.

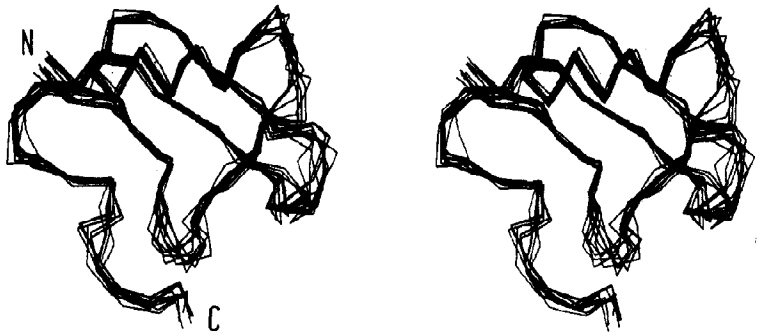

Fig. 6. Computer stereo drawings of the α-pseudoatom backbone of 10 calculated structures of neurotoxin M_9, which are consistent with the NMR data shown in figs. 4, 5, 7 and 9 and table 1. The structures are superimposed so as to minimize the root-mean-square deviation of the α-pseudoatoms with respect to the arbitrarily chosen structure in the calculated set. Positions of the N- and C-termini are indicated. For the sake of clarity, the disulfide bonds are not shown.

β. The pseudoatom α represents the backbone fragment of a residue and β the side chain. Calculations were carried out as described in refs. 8 and 9. In all, 10 structures shown in fig. 6 were computed that are consistent with the NOE and nonbonding distance constraints. The average root-mean-square coordinate deviation between these structures amounts to 0.23 ± 0.03 nm, for α-pseudoatoms being only 0.21 ± 0.02 nm, i.e., they are conformationally similar to one another. Details of the secondary and tertiary structures have been refined by analysis of the experimental data (NOE, vicinal coupling constants, NH rates of exchange) by using the molecular model of neurotoxin M_9.

The spatial structure of the major conformer of M_9 (fig. 7), in accordance with the data obtained (table 1 and fig. 4), contains 2.5 turns of right-handed α-helix (residues 22–31) and a three-stranded antiparallel β-structure (residues 1–5, 46–52 and 35–40). Reverse turns of the polypeptide chain occur in the region of residues 8–11, 18–21, 31–35, 41–45 and, presumably, 61–64. The polypeptide chain also bends at residues 52–54 and 59–61. The peptide NH exchange rates, NOE $^1d_{NN}$ (fig. 4) and coupling constants ^3J(H-NC$^\alpha$-H) of residues Asp-55 and Asn-56 (5 and 7.7 ± 0.4 Hz, respectively) indicate that the conformation in region 54–57 is close to that of a standard type I β-turn [20]. The observed NOE $^1d_{\alpha\delta}$, which is indicative of a *trans* configuration for an X–Pro bond [8], proves that all five X–Pro bonds in the dominant conformer M_9 are in the *trans* configuration (fig. 8).

Because of the low rate of conformational exchange, it may be suggested that the conformational heterogeneity of the neurotoxin M_9 molecule is due to *cis* isomerism of one of the X–Pro peptide bonds in the minor conformer (presumably the Lys^8–Pro^9 bond, according to the signal splittings and the spatial structure obtained for the main conformer).

Analysis of the relative positions of the side chains reveals two hydrophobic clusters on opposite sides of the dominant M_9 conformer globule.

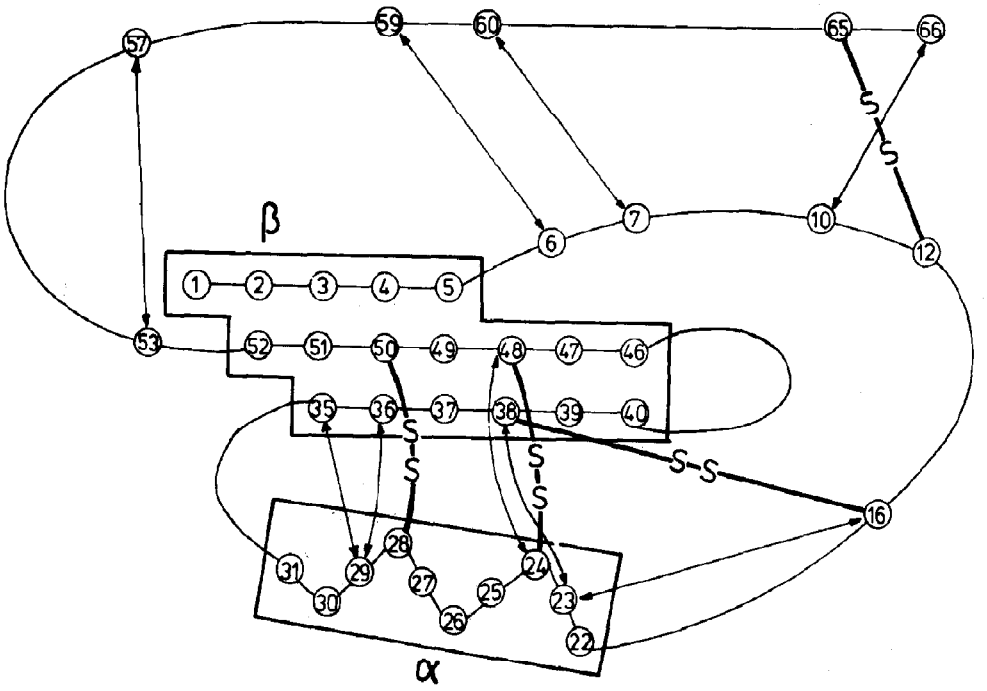

Fig. 7. Schematic representation of the spatial structure of neurotoxin M_9. α, α-helix; β, β-structure. Arrows show sequentially distant proton NOE interactions. Disulfide bridges are indicated.

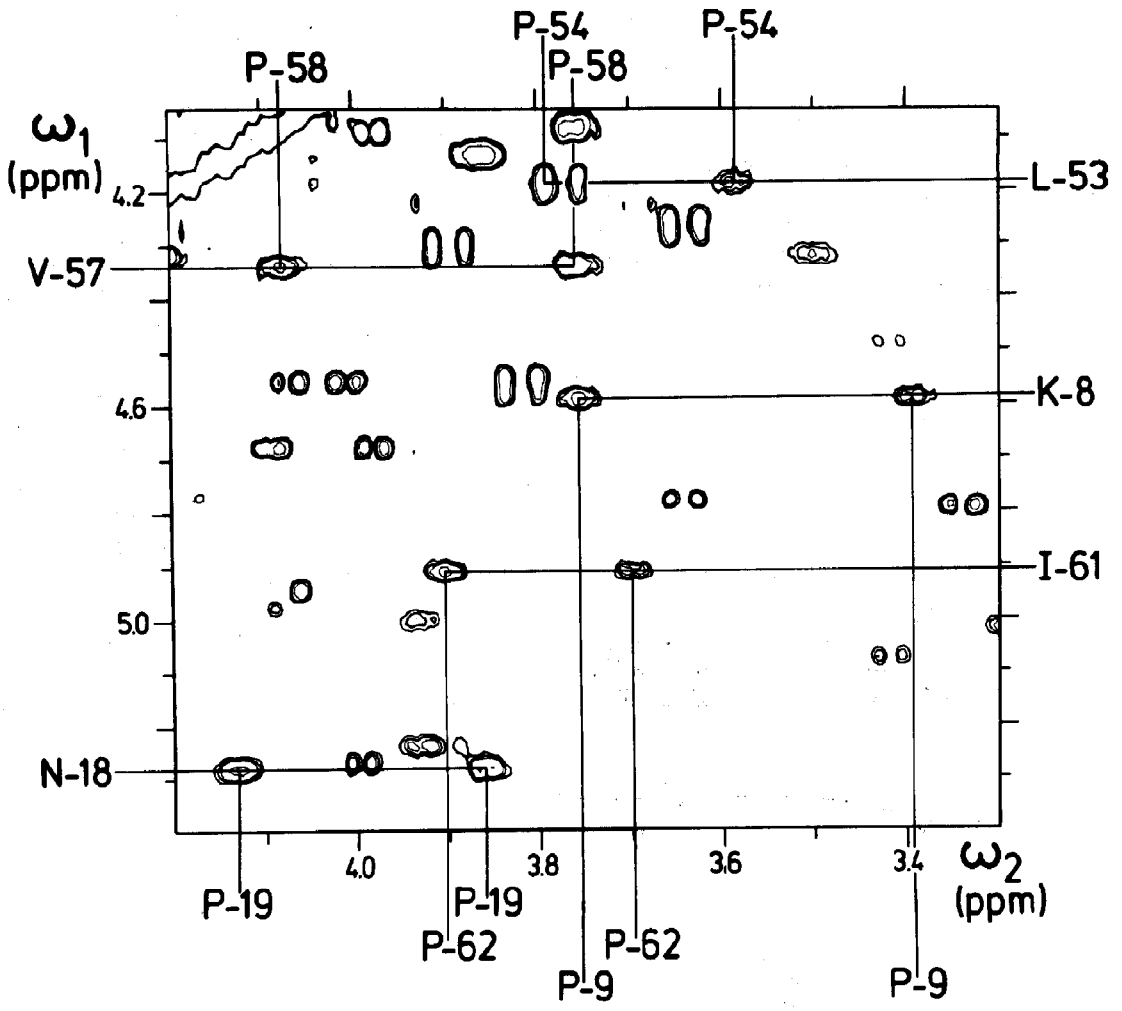

Fig. 8. Contour plot of the region $\omega_1 = 4.05–5.4$ ppm, $\omega_2 = 3.30–4.30$ ppm of the phase-sensitive mode NOESY proton spectrum of neurotoxin M_9 in ^2H_2O at 30 °C and pH 2.8. Proline $C^\delta H_2$ proton chemical shifts are indicated at the top and bottom, while those of the $C^\alpha H$ protons of the preceding residues in the primary structure are given on the left- and right-hand sides.

One of them includes the side chains of residues 5, 37, 44, 49, 51 and 59 (fig. 9A). Another, smaller cluster contains the side chains of residues 6, 14, 23 and 27 (fig. 9B).

4. Discussion

For molecules with a definite, dominant conformation, it is customary to represent the three-dimensional structure as if it were a rigid frame, although it is obvious that in solution, the molecules are subject to some degree of intramolecular motion.

Comparison of the three-dimensional structures of neurotoxin M_9 and insectotoxins v-3 [3,4] and I_{5A} [2,6–9] shows apparently the same conformational motif in their spatial organization, i.e., a similar orientation of the α-helix relative to the β-sheet (fig. 10). Particularly close correspondence is seen between the spatial structures of neurotoxin M_9 and insectotoxin v-3, although they share a poor sequence homology. This provides experimental proof of the previous theoretical sugges-

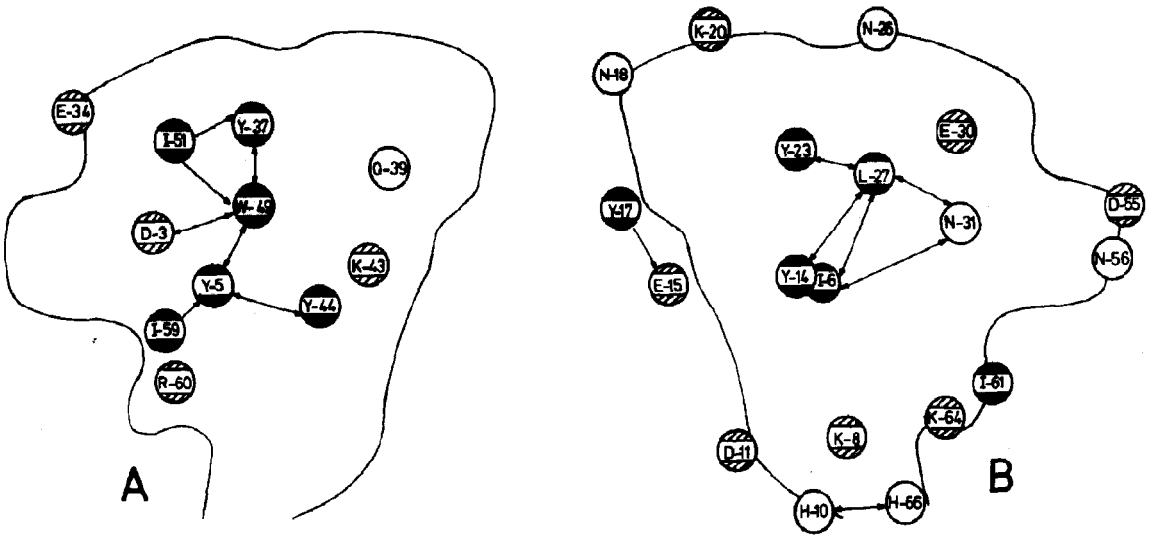

Fig. 9. Schematic representation of the amino acid side chain distribution on the surface of the dominant conformer of neurotoxin M_9. Same view as presented in figs. 6 and 10 (A) and rearward view (B). Hydrophobic side chains are shown as filled areas; charged side chains are indicated by the hatched areas. Arrows indicate experimentally established NOE interactions between protons of the side chains.

tion that the 'long' scorpion toxins have similar three-dimensional structures [3,4]. Aside from the cystine residues, there are only three small conserved regions in the primary structures of long scorpion toxins (fig. 11). Most of these conserved side chains are located on the same side of the molecular surface (fig. 9A), which, as suggested previously [3,4], may be directly involved in inter-

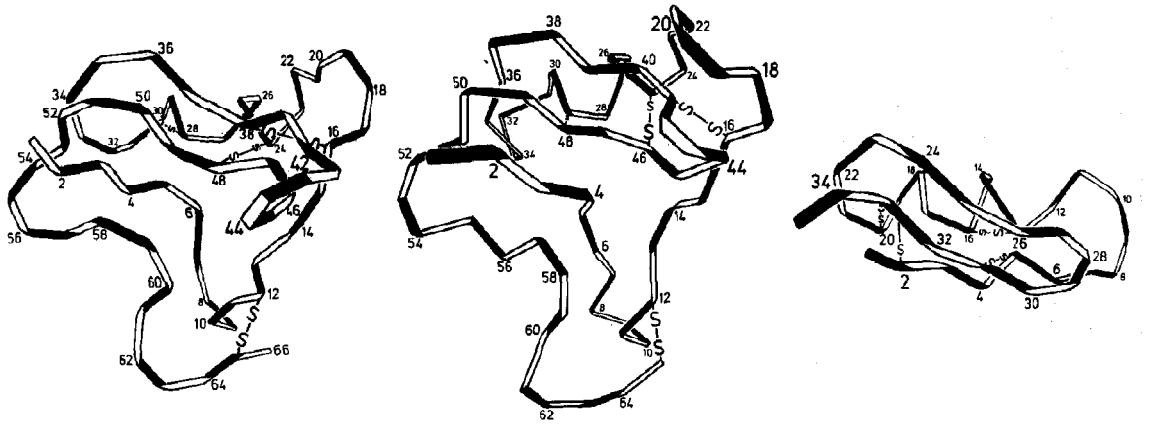

Buthus eupeus *Centruroides sculpturatus* *Buthus eupeus*

Fig. 10. Backbone folding of the dominant conformer of M_9, v-3 [3,4] and I_{5A} [2,6–9] scorpion toxins. The latter two structures have been redrawn from the respective references cited.

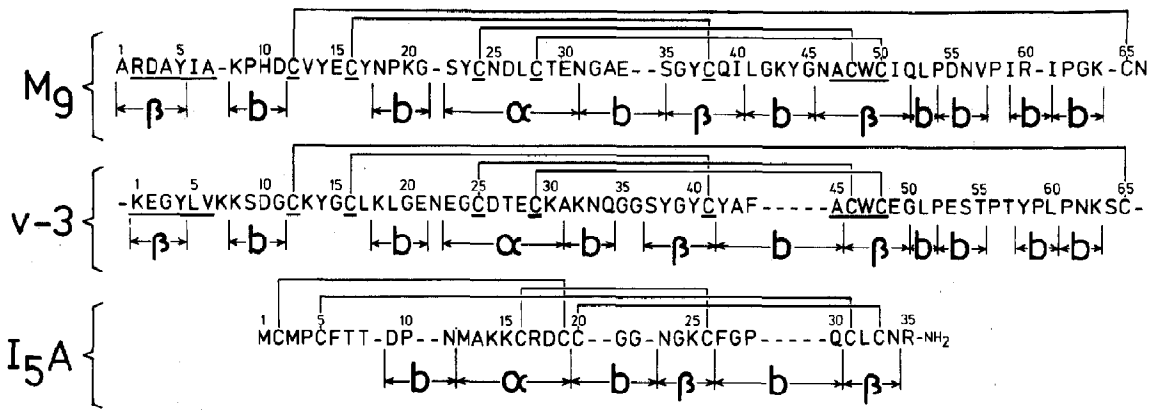

Fig. 11. Amino acid sequences of the three scorpion toxins aligned to achieve maximum correspondence in distribution of secondary structural elements; α, α-helix; β, β-strand; b, bend in the backbone direction. Amino acid residues invariant or conserved in the primary structures of the long scorpion toxin are underlined.

action with the Na^+ channels of an excitable membrane. This suggestion is experimentally confirmed by the present study, in that the 'long' scorpion toxins possess similar spatial structures. In addition, interaction of the photosensitive derivative of the mammalian scorpion toxin with Na^+-channel preparations [2] reveals a contact between the Na^+ channel and the side chain of a residue equivalent to Arg-60 in the primary structure of neurotoxin M_9 (figs. 10 and 11) located at the surface of the molecule.

By analogy with the interaction between the acetylcholine receptor and snake neurotoxins [2,21], the high affinity of the mammalian and scorpion toxins for Na^+ channels ($K_d \sim 10^{-9}$ M [22]) allows one to suggest a multipoint nature for this interaction and indicates that the mammalian scorpion toxin-binding site is quite extended. In this respect, it is worthwhile to consider some other experimental results. Firstly, a four-stranded antiparallel β-sheet has been demonstrated in sea anemone neurotoxins, which apparently compete with mammalian scorpion toxins for a common Na^+-channel-binding site [23]. The relative position of the strands of this β-structure resembles the polypeptide chain folding of neurotoxin M_9 (the β-sheet and the initial part of the C-terminal fragment; see fig. 10). Secondly, chemical modifications of mammalian scorpion toxins show that the toxicity and/or affinity for Na^+ channels are decreased substantially upon cleavage of a single disulfide bond [24] or by elimination of positive charges from side chains of the amino acid residues [25], which are equivalent to residues 2 and 60 in the primary structure of neurotoxin M_9 (figs. 10 and 11). Thirdly, interaction between the Na^+-channel preparations and photosensitive derivatives of the mammalian scorpion toxins [26] indicates that the side chain of the amino acid residue, equivalent to residue 64 in the primary structure of M_9, is involved in a contact with the Na^+-channel surface of the complex formed.

From the above evidence and the structures of the scorpion toxins shown in figs. 10 and 11, differences in the biological activities of neurotoxin M_9 and insectotoxin I_{5A} could be attributed to the presence of additional amino acid residues in the primary structure of M_9 (residues 1–9 and 50–66). In the case of M_9 and v-3, the difference might be related to the amino acid substitutions in the corresponding positions of the tertiary structures. For instance, the positively charged side chain of Arg-60, which is essential for the biological activity of the mammalian scorpion neurotoxins [25], is replaced by the hydrophobic Tyr-58 side chain in the structure of insectotoxin v-3 (fig. 11).

Thus, the interaction of neurotoxin M_9 with Na^+ channels probably involves a number of the side chains of neurotoxin M_9, located spatially

near Arg-60 in the β-sheet and C-terminal part of the molecule.

References

1 H. Rochat, P. Bernard and F. Couraud, in: Advances in Cytopharmacology, eds. B. Ceccarelli and F. Clementi, vol. 3 (Raven Press, New York, 1979) p. 325.
2 Yu.A. Ovchinnikov, Pure Appl. Chem. 56 (1984) 1049.
3 R.J. Almassy, J.C. Fontecilla-Camps, F.L. Suddath and C.E. Bugg, J. Mol. Biol. 170 (1983) 497.
4 A. Zell, S.E. Ealick and C.E. Bugg, in: Molecular architecture of proteins and enzymes, eds. R.A. Bradshaw and J. Tang (Academic Press, New York, 1985) p. 65.
5 N.R. Krishna, C.E. Bugg, R.L. Stephens and D.D. Watt, J. Biomol. Struct. Dyn. 1 (1983) 829.
6 A.S. Arseniev, V.I. Kondakov, V.N. Maiorov, T.M. Volkova, E.V. Grishin, V.F. Bystrov and Yu.A. Ovchinnikov, Bioorg. Khim. 9 (1983) 768.
7 V.F. Bystrov, A.S. Arseniev, V.I. Kondakov, V.N. Maiorov, V.V. Okhanov and Yu.A. Ovchinnikov, in: Toxins as tool in neurochemistry, eds. F. Hucho and Yu.A. Ovchinnikov (De Gruyter, Berlin, 1983) p. 291.
8 A.S. Arseniev, V.I. Kondakov, V.N. Maiorov and V.F. Bystrov, FEBS Lett. 165 (1984) 57.
9 V.N. Maiorov, A.S. Arseniev and V.F. Bystrov, Bioorg. Khim. 11 (1985) 1192.
10 M.J. Dufton, A.F. Drake and H. Rochat, Biochim. Biophys. Acta 869 (1986) 16.
11 T.M. Volkova, A.F. Garsia, I.N. Telezhinskaya, N.A. Potapenko and E.V. Grishin, Bioorg. Khim. 11 (1985) 1445.
12 G. Wider, S. Macura, A. Kumar, R.R. Ernst and K. Wüthrich, J. Magn. Reson. 56 (1984) 207.
13 A.Z. Gurevich, I.L. Barsukov, A.S. Arseniev and V.F. Bystrov, J. Magn. Reson. 56 (1984) 471.
14 G. Wagner and K. Wüthrich, J. Mol. Biol. 155 (1982) 347.
15 D. Neuhaus, G. Wagner, M. Vašák, J.H.R. Kägi and K. Wüthrich, Eur. J. Biochem. 151 (1985) 257.
16 M. Billeter, W. Braun and K. Wüthrich, J. Mol. Biol. 155 (1982) 321.
17 V.S. Pashkov, A.N. Hoang, V.N. Maiorov and V.F. Bystrov, Bioorg. Khim. 12 (1986) 1306.
18 Anil Kumar, G. Wagner, R.R. Ernst and K. Wüthrich, J. Am. Chem. Soc. 103 (1981) 3654.
19 W. Braun, C. Bösch, L.R. Brown, N. Gō and K. Wüthrich, Biochim. Biophys. Acta 667 (1981) 377.
20 G. Wagner, D. Neuhaus, E. Wörgötter, M. Vašák, J.H.R. Kägi and K. Wüthrich, J. Mol. Biol. 187 (1986) 131.
21 V.I. Tsetlin, E. Karlsson, A.S. Arseniev, Yu.N. Utkin, A.M. Surin, V.S. Pashkov, K.A. Pluzhnikov, V.T. Ivanov, V.F. Bystrov and Yu.A. Ovchinnikov, FEBS Lett. 106 (1979) 47.
22 E. Jower, N. Martin-Moutot, F. Couraud and H. Rochat, Biochemistry 19 (1980) 463.
23 P.R. Gooley and R.S. Norton, Biochemistry 25 (1986) 2349.
24 C. Habersetzer-Rochat and F. Sampiery, Biochemistry 15 (1976) 2254.
25 H. Darbon, E. Jover, F. Couraud and H. Rochat, Int. J. Peptide Protein Res. 22 (1983) 179.
26 Yu.N. Utkin, E.M. Lasakovich, A.A. Kaydalov, E.V. Grishin and V.I. Tsetlin, in: Synaptic transmitters and receptors, ed. S. Tuček (Academia, Praha, 1987) p. 422.